Supplemental materials

Genomic analysis of Rad26 and Rad1-Rad10 reveals differences in their dependence on Mediator and RNA polymerase II

Diyavarshini Gopaul, Cyril Denby Wilkes, Arach Goldar, Nathalie Giordanengo Aiach, Marie-Bénédicte Barrault, Elizaveta Novikova and Julie Soutourina

Supplemental Table S1. Yeast strains used in the study.

Collection #	Strain Name	Genotype
Y0097	YPH499 WT	*MATa ura3-52 his3-Δ200 ade2-101uaa trp1-Δ63 lys2-801uag leu2-Δ1*
Y6611	BY4741 WT	*MATa his3-Δ1 leu2Δ-0 met15Δ-0 ura3Δ-0*
Y6612	BY4742 WT	*MATα his3Δ-1 leu2Δ-0 lys2Δ-0 ura3Δ-0*
Y6244	YPH499 rad26Δ	*MATa ura3-52 his3-Δ200 ade2-101uaa trp1-Δ63 lys2-801uag leu2-Δ1 rad26::KanMX6*
Y7726	BY4742 rad26Δ	*MATα his3Δ-1 leu2Δ-0 lys2Δ-0 ura3Δ-0 rad26::KanMX6*
Y6245	YPH499 rad7Δ	*MATa ura3-52 his3-Δ200 ade2-101uaa trp1-Δ63 lys2-801uag leu2-Δ1 rad7::HIS3*
Y7116	BY4742 rad7Δ	*MATα his3Δ-1 leu2Δ-0 lys2Δ-0 ura3Δ-0 rad7::KanMX6*
Y6247	YPH499 rad26Δ rad7Δ	*MATa ura3-52 his3-Δ200 ade2-101uaa trp1-Δ63 lys2-801uag leu2-Δ1 rad26::KanMX6 rad7::HIS3*
Y7727	BY4742 rad26Δ rad7Δ	*MATα his3Δ-1 leu2Δ-0 lys2Δ-0 ura3Δ-0 rad26::KanMX6 rad7::HIS3*
Y7314	YPH499 rad10Δ	*MATa ura3-52 his3-Δ200 ade2-1 trp1-Δ63 lys2-801uag leu2-Δ rad10::hph*
Y6191	BY4741 rad10Δ	*MATa his3-Δ leu2Δ-0 met15Δ-0 ura3Δ-0 rad10::KanMX4*
Y7313	YPH499 rad1Δ	*MATa ade2-1 lys2-801 ura3-52 trp1-Δ63 his3-Δ200 leu2-Δ rad1::hph*
Y6187	BY4741 rad1Δ	*MATa his3-Δ1 leu2Δ-0 met15Δ-0 ura3Δ-0 rad1::KanMX4*
Y4582	dst1Δ	*MATa lys2-801 trp1-Δ63 his3-Δ200 leu2-Δ1 dst1::KanMX4*
Y6200	Rad1-HA	*MATa ura3-52 his3-Δ200 ade2-101uaa trp1-Δ63 lys2-801uag leu2-Δ1 RAD1::3HA::HIS3*
Y6201	HA-Rad1	*MATa ura3-52 his3-Δ200 ade2-101uaa trp1-Δ63 lys2-801uag leu2-Δ1 HIS3::pADH1::3HA::RAD1*
Y6204	Rad10-HA	*MATa ura3-52 his3-Δ200 ade2-101uaa trp1-Δ63 lys2-801uag leu2-Δ1 RAD10::3HA::HIS3*
Y7064	Rad10-Flag	*MATa ade2-1 lys2-801 ura3-52 trp1-Δ63 his3-Δ200 leu2Δ RAD10::3Flag::KanMX4*
Y6572	HA-Rad1 Med17-Myc	*MATa ura3-52 his3-Δ200 ade2-101uaa trp1-Δ63 lys2- Δ1 leu2-Δ1 HIS3::pADH1::3HA::RAD1 MED17::13MYC::TRP1*
Y7061	Rad10-Flag Med17-Myc	*MATα ura3-52 his3-Δ200 ade2-101uaa trp1-Δ63 lys2- 801uag leu2-Δ1 RAD10::3Flag::KanMX4 MED17::13MYC::TRP1*
Y7050	HA-Rad26	*MATa ade2-1 lys2-801 ura3-52 trp1-Δ63 his3-Δ200 leu2Δ HIS3::HA::RAD26*
Y7194	HA-Rad26 Med17-Myc	*MATa ade2-1 lys2-801 ura3-52 trp1-Δ63 his3-Δ200 leu2Δ HIS3::HA::RAD26 MED17::13MYC::TRP1*
Y7629	rpb1-1 Rad10-HA	*MATα ura3-52 leu2-Δ1 his3-Δ200 trp1-Δ63 rpb1-1(rpb1-G1437D) RAD10::3HA::HIS*
Y7628	rpb1-1 Rad1-HA	*MATα ura3-52 leu2-Δ1 his3-Δ200 trp1-Δ63 rpb1-1(rpb1-G1437D) RAD1::3HA::HIS3*
Y7117	Rad26-HA rad7Δ	*MATa ura3-52 his3-Δ200 ade2-101uaa trp1-Δ63 lys2-801uag leu2-Δ1 RAD26::3HA::KanMX6 rad7::HIS*
Y7118	HA-Rad26 rad7Δ	*MATa ade2-1 lys2-801 ura3-52 trp1-Δ63 his3-Δ200 leu2Δ HIS3::HA::RAD26 rad7::KAN*
Y6202	Rad14-HA	*MATa ura3-52 his3-Δ200 ade2-101uaa trp1-Δ63 lys2-801uag leu2-Δ1 RAD14::3HA::HIS3*
Y6203	HA-Rad14	*MATa ura3-52 his3-Δ200 ade2-101uaa trp1-Δ63 lys2-801uag leu2-Δ1 HIS3::pADH1::3HA::RAD14*

Y6578	Rad4-HA	*MATa ade2-1 lys2-801 ura3-52 trp1-Δ63 his3-Δ200 leu2Δ RAD4::HA::HIS3*
Y6579	HA-Rad4	*MATa ade2-1 lys2-801 ura3-52 trp1-Δ63 his3-Δ200 leu2Δ HIS3::HA::RAD4*
Y6573	Rad14-HA Med17-Myc	*MATa ura3-52 his3-Δ200 ade2-101uaa trp1-Δ63 lys2- 801uag leu2-Δ1 RAD14::3HA::HIS3 MED17::13MYC::TRP1*
Y6574	HA-Rad14 Med17-Myc	*MATa ura3-52 his3-Δ200 ade2-101uaa trp1-Δ63 lys2- 801uag leu2-Δ1 HIS3::pADH1::3HA::RAD14 MED17::13MYC::TRP1*
Y6604	Rad4-HA Med17-Myc	*MATa ade2-1 lys2- 801 ura3-52 trp1-Δ63 his3-Δ200 leu2-Δ l RAD4::3HA::HIS3 MED17::13MYC::TRP1*
Y6605	HA-Rad4 Med17-Myc	*MATa ade2-1 lys2-801 ura3-52 trp1-Δ63 his3-Δ200 leu2-Δ HIS3::pADH1::3HA::RAD4 MED17::13MYC::TRP1*
Y6300	YPH500 Med17-Myc	*MATα ura3-52 his3-Δ200 ade2-101uaa trp1-Δ63 lys2-801uag leu2-Δ1 MED17::13MYC::TRP1*
Y7751	YPH499 Med17-Myc	*MATa ura3-52 his3-Δ200 ade2-101uaa lys2-801uag leu2-Δ1 MED17::13Myc::TRP1*
Y7641	Rad10-HA rpc25-S100P	*MATa ura3-52 trp1-Δ63 his3- 200 leu2- Δ1 ade2-101uaa lys2-801 ade2-1 rpc25-S100P RAD10::3HA::HIS3*
Y7639	Rad10-Flag rad2Δ	*MATα ura3-52 his3- Δ200 ade2-101uaa trp1-Δ63 lys2-801uag leu2-Δ1 rad2::KanMX6 RAD10::3Flag::hph*
Y7734	Rad10-HA Med5-Myc MED17-WT	*MATa ura3-52 his3-Δ200 ade2-101uaa trp1-Δ63 lys2-801uag leu2-Δ1 Med17::kan::ADE2 MED5::13Myc::KanMX6 RAD10::3HA::HIS3 CEN MED17 LEU2*
Y7735	Rad10-HA Med5-Myc med17-138	*MATa ura3-52 his3-Δ200 ade2-101uaa trp1-Δ63 lys2-801uag leu2-Δ1 med17::kan::ADE2 MED5::13Myc::KanMX6 RAD10::3HA::HIS3 CEN med17-138 LEU2*
Y7730	HA-Rad26 Med5-Myc MED17-WT	*MATa ura3-52 his3-Δ200 ade2-101uaa trp1-Δ63 lys2-801uag leu2-Δ1 med17::kan::ADE2 MED5::13Myc::KanMX6 HIS ::3HA::RAD26 CEN MED17 LEU2*
Y7731	HA-Rad26 Med5-Myc med17-138	*MATa ura3-52 his3-Δ200 ade2-101uaa trp1-Δ63 lys2-801uag leu2-Δ1 med17::kan::ADE2 MED5::13Myc::KanMX6 HIS ::3HA::RAD26 CEN med17-138 LEU2*
Y7666	Rad10-HA Med17-Myc KIN28-WT	*MATα ade2-1 lys2-801uag ura3-52 trp1-Δ63 his3-Δ200 leu2-Δ RAD10::3HA::HIS3 MED17::13Myc::TRP1 kin28::KanMX6 CEN KIN28 LEU2*
Y7667	Rad10-HA Med17-Myc kin28-ts16	*MATα ade2-1 lys2-801uag ura3-52 trp1-Δ63 his3-Δ200 leu2-Δ RAD10::3HA::HIS3 MED17::13Myc::TRP1 kin28::KanMX6 CEN kin28-ts16 LEU2*
Y7668	HA-Rad26 Med17-Myc KIN28-WT	*MATα ade2-1 lys2-801uag ura3-52 trp1-Δ63 his3-Δ200 leu2-Δ HIS3::3HA::RAD26 MED17::13Myc::TRP1 kin28::KanMX6 CEN KIN28 LEU2*
Y7669	HA-Rad26 Med17-Myc kin28-ts	*MATα ade2-1 lys2-801uag ura3-52 trp1-Δ63 his3-Δ200 leu2-Δ HIS3::3HA::RAD26 MED17::13Myc::TRP1 kin28::KanMX6 CEN kin28-ts16 LEU2*
Y6960	Rad1-HA Med17-Myc KIN28-WT	*MATa ura3-52 his3-Δ200 ade2-101uaa trp1-Δ63 lys2-801uag leu2-Δ1 RAD1::3HA::HIS3 MED17::13Myc::TRP1 kin28::KanMX6 CEN KIN28 LEU2*
Y6961	Rad1-HA Med17-Myc kin28-ts16	*MATa ura3-52 his3-Δ200 ade2-101uaa trp1-Δ63 lys2-801uag leu2-Δ1 RAD1::3HA::HIS3 MED17::13Myc::TRP1 kin28::KanMX6 CEN kin28ts16 LEU2*
Y7196	Rad2-HA Med17-Myc rad10Δ	*MATα ade2-1 lys2-801 ura3-52 trp1-Δ63 his3-Δ200 leu2-Δ HIS3::pADH1::3HA::RAD2 rad10::KanMX6 MED17::13Myc::TRP1*
Y7195	Rad2-HA Med17-Myc rad1Δ	*MATα ade2-1 lys2-801 ura3-52 trp1-Δ63 his3-Δ200 leu2-Δ HIS3::pADH1::3HA::RAD2 rad1::KanMX6 MED17::13Myc::TRP1*
Y7752	Med17-Myc rad26Δ	*MATa ura3-52 his3-Δ200 ade2-101uaa trp1-Δ63 lys2-801uag leu2-Δ1 rad26::KanMX6 MED17::13Myc::TRP1*

Supplemental Table S2. qPCR primers used in the study.

Name	Forward	Reverse
ADH1-U	ATAGGCGCATGCAACTTCTT	CATCAGCTCTGGAACAACGA
CLN1-U	ATTCCCTTGTTCGCAACACT	CGCGGGGTTGTAGTAGGTAA
LEU1-U	CGTCATAATAGTTCCTGCCCAGCT	TGTATCTTGAGTGTCTGTATGGGCG
PCL1-U	GGCTCTAGTGTTCTGCGAATG	ACATTTCGAGTCGCTTTTGC
PDR5-U	AAGACTGCCCCTCTCTTTCC	AAGACTGCCCCTCTCTTTCC
PMA1-U	AACAAACCCGGTCTCGAAG	GAAGTGCCGCATTAGGAAAT
PYK1-U	CACCGTCACAAAGTGTT	TGGGAAGGAAAGGAAATCAC
SSF2-U	GCGAATGGCTTGTGAAACAAACA	TGCAAGTGCTTAGGTCTGTTTGG
OLE1-U	TGACAGGCAGAGGTAATAACGG	AAGACTCGTAGAAGCACACCTG
PCK1-U	CAATTCTGACCAGAGCACTTGG	CAGATCTCCATTCACCCGTCAG
ADH1-P	TTCCTTCATTCACGCACACT	AGGGAACGAGAACAATGACG
PMA1-P	GATGGTGGGTACCGCTTATG	TTGGTGTTATAGGAAAGAAAGAGAAAA
PYK1-P	CCTTTCCTTCCCATATGATGC	ACTTTGAAAGGGGACCATGA
SGV1-P	CGCGTCGAACGGAAATACACCC	CTGCTTGACCACGAATGTACTGC
ADH1-O	GGCTGGAAGATCGGTGACTA	TCAGCGGTAGCGTATTGTTG
BRF2-O	GGTGGAAAAGTCTAAGTTAAGAGCAG	CGTCCTCATTCTCGGAAACTTC
GAL1-O	AAAGAAACTTGCACCGGAAA	GGCCCATATTCGCTTTAACA
PDR5-O	CTCCAGGCTATGACCCAAAA	GTTCTTCCAAGCGCAACCTA
PMA1-O	TCTCCAAAGCCCGTTAAATG	CGTTCATAGCACCGAAGTT
PYK1-O	ATGGTTGCCAGAGGTGACTT	TCTGGTTGGTCTTGGGTTGT
TPI1-O	TAACGTCGTTGTCGCTTACG	CCAACTTGGAAGCCAAGAAC
RAD2-O	TGAGTCTTCTAACGCGACGA	TAAGGCAACCTTGCAGCTTT
IGV	TTCATTTGCAATTTGCAGTTCA	CAGCCAGGAAGAATCTCACAA
TEL1R	TCAACTACCCTCCCTCTCCAT	GTGGAGTGGGGGAATGAGAC
TEL1R-XC1	CATCTATCCCCTGCCCAATA	ACGTGGTAGATGGGGATTGT
RPR1	ATGGTACGCTGTGGTGCTC	CCATAGGTGGGGATCCTTCT
tDNAMet	GCTTCAGTAGCTCAGTAGGAA	TGCTCCAGGGGAGGTTC
tDNAPhe	GACGCTTGGACCATTTATAAAGCAC	CCATAAGAGAAGGAGCAGTCAAGTTCA
SCR1	ACCGCTGTTAGGGGAGTTTT	CCAAATTAAACCGCCGAAG

Supplemental Table S3. Number of mapped and unique reads, and normalization coefficients in ChIP-seq experiments.

Name	Unique mapped reads	Average Insertion Size	Normalization Factor
Input_Kin28WT	27621977	321	1
Input_Kin28TS	22653444	309	1
Rad26_Kin28WT	20512333	250	1
Rad26_Kin28TS	15914202	218	1.6515
Med17_Kin28WT	13479060	191	1
Med17_Kin28TS	9728462	205	0.9861
Pol2_Kin28WT	20472442	249	1
Pol2_Kin28TS	20810040	199	3.9843
Rad1_Kin28WT	13949359	216	1
Rad1_Kin28TS	8367165	175	0.8090
Rad10_Kin28WT	18118057	198	1
Rad10_Kin28TS	17453391	186	0.7715

Supplemental analysis

Concomitant analysis of Mediator, Rad1, Rad10, Rad26 and Pol II genomic coverage signal on intergenic regions

To investigate in detail the complex relationship between different NER proteins and transcriptional components that co-occupy intergenic regions, we analyzed simultaneously the genome-wide data sets for Mediator, Pol II, Rad1, Rad10 and Rad26 in wild type and *kin28* mutant contexts. To this aim, it is necessary to define a frame of reference where the variables can be positioned independently of each other. To define such an abstract coordinate system where we can measure the orientation and distances between different variables, we decompose the data sets into principal components. Principal component analysis (PCA) for multivariate systems evaluates the variability in data sets with a reduced number of parameters and constructs an orthonormal coordinate system, where the orthogonal directions are statistically independent. Pareto representation showed that three principal components (PCs) are sufficient to explain 94.1% or 92.4% of the data variability in the wild type and the *kin28* mutant, respectively (**Supplemental Figure S14A**). The space of three PCs (orthonormal referential $\{PC_1, PC_2, PC_3\}$) was thus considered in further analysis (**Supplemental Figure S15)**. To understand how different variables (Mediator, Pol II, Rad1, Rad10 and Rad26) participate in the construction of PCs, the norm of each variable was calculated (**Supplemental Figure S14B**). In the wild type, Mediator contributes the most to the observed data set variability, followed closely by Rad26, Pol II, Rad1 and Rad10. However, in the *kin28* mutant Pol II contributes the most to the observed data set variability, followed closely by Mediator, Rad26, Rad1 and Rad10. We then measured the contribution of each variable to each PC (**Supplemental Figure S14C**). This analysis showed that Rad1 and Rad10 proteins are the main contributors to PC1 in the wild type, whereas in the *kin28* mutant the main contributors are Rad10 and Rad26. The PC2 is mainly influenced by Mediator and Pol II in the wild type,

whereas the *kin28* mutation changes the main contribution to Mediator and Rad1. The three proteins Rad26, Rad1 and Rad10 are the main contributors to the definition of PC3 in the wild type, whereas Rad26 and Pol II influenced the most this PC in the *kin28* mutant. Therefore, the stabilization of Mediator in the *kin28* mutant affects mainly the interplay between Rad1-Rad10 and Rad26 proteins, and between Rad26 and Pol II.

We also calculated the covariance between variables by projecting one variable over the other in the orthonormal reference of the three PCs (**Supplemental Figure S16A, B**), and plotted the covariance between the variables for the wild type and the *kin28* mutant (**Supplemental Figure S16C**). This ellipsoid representation illustrates the correlation or anti-correlation relationship between variables. The width of the ellipsoid (small radius) corresponds to the dispersion of the relation between the two variables. To illustrate how the *kin28* mutation changes the relationship between variables, the ellipsoid contours of the covariance distribution were compared between the wild type and the *kin28* mutant on the intergenic regions by plotting them on the same graph and by indicating differences of covariance between mutant and wild type (**Supplemental Figure S16C**).

In both contexts, we observed a strong correlation between Rad1 and Rad10 on intergenic regions (0.95 and 0.84, respectively, **Supplemental Figure S16A, B**), in accordance with the existence of a stable Rad1-Rad10 dimer. The *kin28* mutation increases dispersion between variables, that is particularly well observed by the increase in the size of the small radius of the ellipsoid representing covariance distribution between Rad1 and Rad10 (**Supplemental Figure S16C**).

This comparison clearly shows that the covariance distribution between Pol II and Rad1, or between Rad26 and Mediator, did not change the orientation in the *kin28* mutant compared to the wild type, whereas the *kin28* mutation leads to an opposite orientation between Rad26 and Pol II, Rad1 or Rad10. Important changes between the *kin28* mutant and the wild type were

observed for several covariances. Our analysis shows a stronger correlation in the mutant between Mediator and Rad26 (0.55 in the *kin28* mutant versus 0.22 in the wild type, positive difference of 0.33 between the mutant and the wild type). In the *kin28* mutant, Rad26 becomes correlated with Rad10 and Rad1, and anticorrelated with Pol II, while the correlation between Rad1-Rad10 and Mediator is reduced (Rad10 loses its correlation with Mediator and Rad1 becomes anti-correlated). Therefore, the stabilization of Mediator on the chromatin in the *kin28* mutant changes considerably the relationship between Mediator, Pol II and Rad26, Rad1-Rad10; in particular it enhances the correlation of Mediator and Rad1-Rad10 with Rad26, and leads to an anti-correlation between Pol II and Rad26.

In conclusion, by taking advantage of the orthonormal referential that one can construct using Principal Component analysis, we formulated a data representation that shows the simultaneous relations on the coverage of the chromatin by different interacting proteins. This representation allowed us to underscore a strong covariance between Rad1 and Rad10, in accordance with their action as a dimer, and a strong correlation between their genome-wide occupancy. Moreover, this analysis improved our understanding of the Rad26 relationship with Mediator and Rad1-Rad10 by revealing the increase in the covariance between Rad26 and Mediator or Rad1-Rad10 that accompanies Mediator stabilization at core promoters.

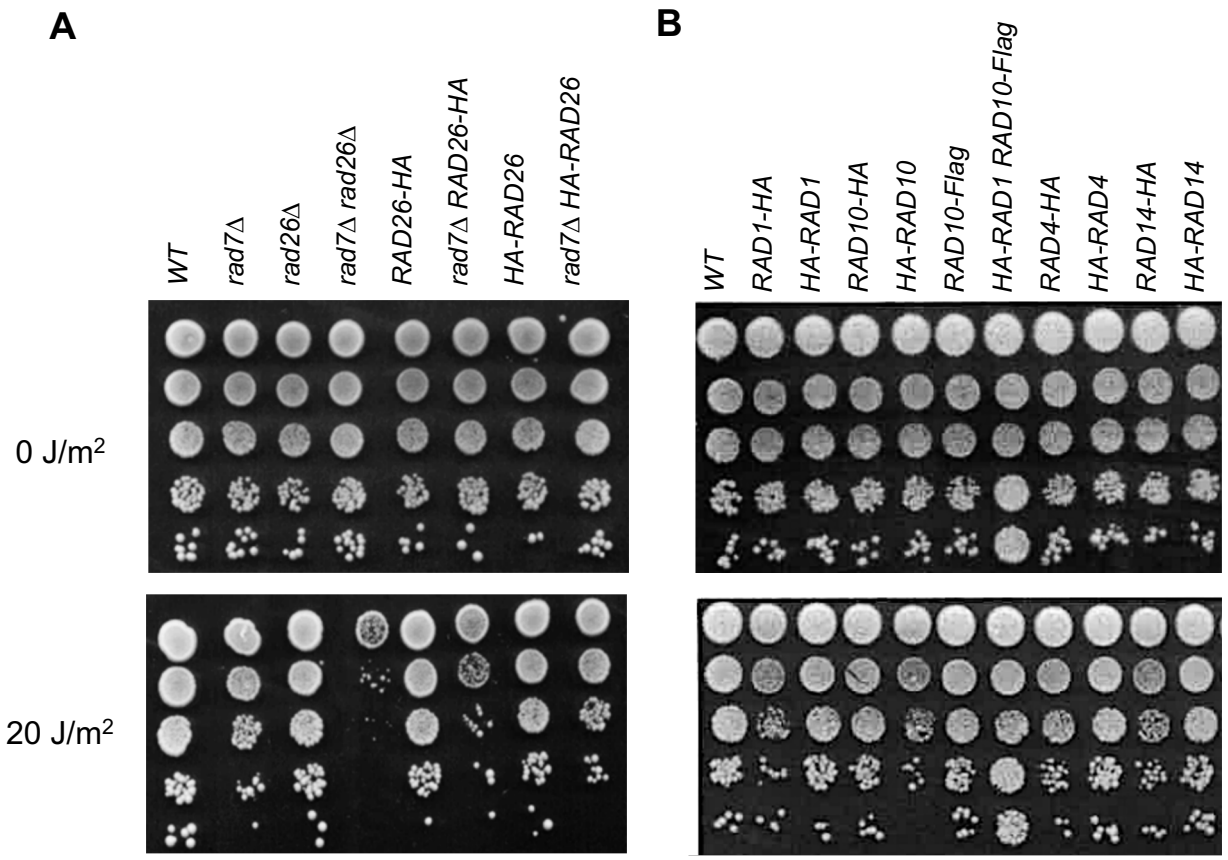

Supplemental Figure S1. UV-sensitivity of *rad26* deletion and Rad26, Rad1, Rad10, Rad4 and Rad14-tagged strains.

Wild-type and isogenic deletion or tagged strains for Rad26 (GGR-proficient or deficient *rad7*Δ contexts, **A**) or tagged strains for Rad1, Rad10, Rad4 and Rad14 (**B**) were serially diluted, spotted on rich-medium YPD agar plates, treated or not with 20J/m^2 of UV (UV Stratalinker 1800) and incubated for 3 days at 30°C. The UV sensitivity of Rad26 strains was tested in a GGR-deficient context, since *rad26* deletion alone did not lead to UV sensitivity in yeast. Rad1-Rad10 are common for both NER subpathways and the UV sensitivity of Rad1-Rad10 tagged strains can thus be tested in a wild-type context.

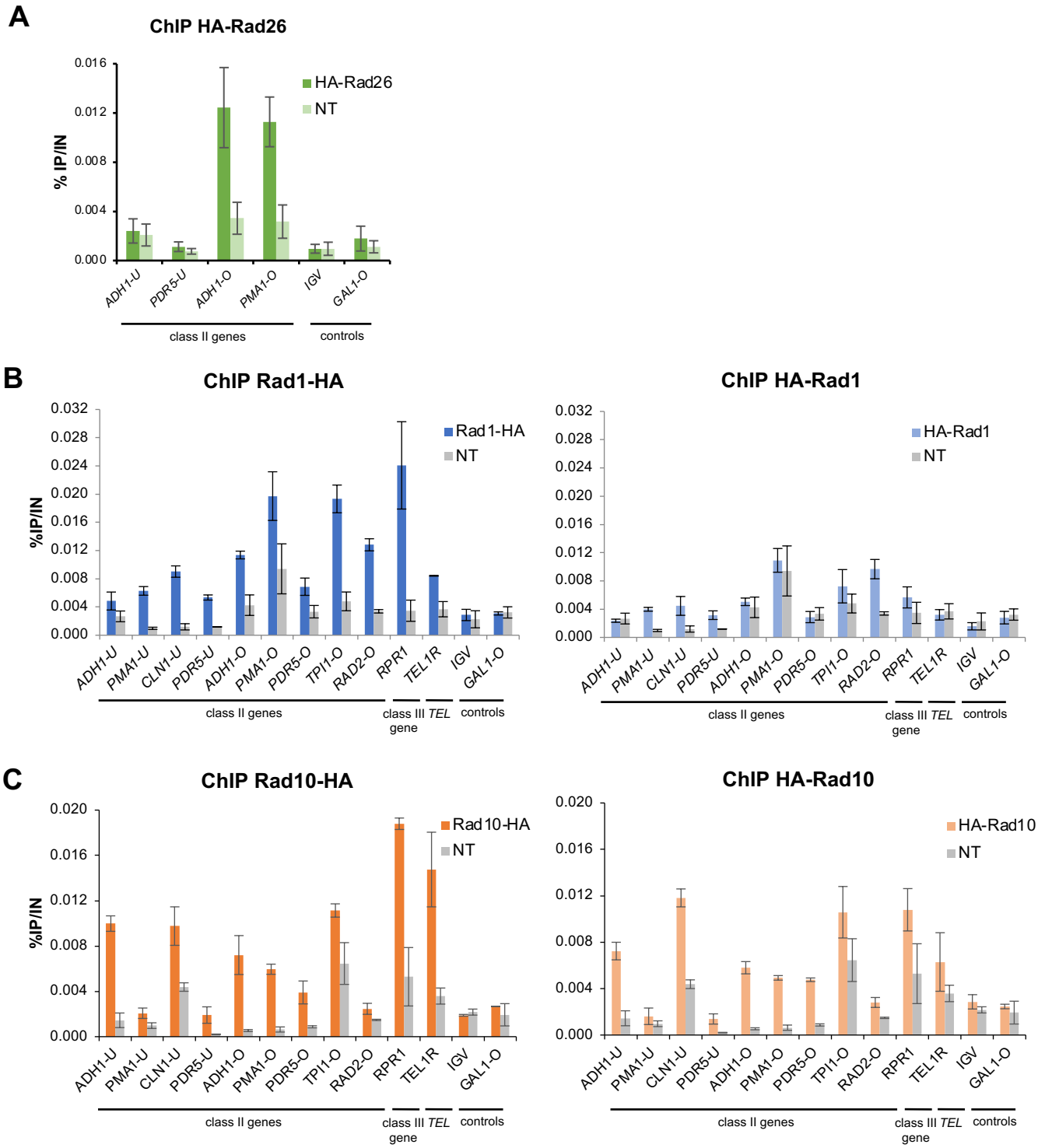

Supplemental Figure S2. ChIP analysis of Rad26, Rad1 and Rad10 occupancy at selected regions.

Quantitative ChIP analysis of Rad26, Rad1 and Rad10 occupancy was performed with α-HA antibody against HA-tagged Rad26 (**A**), Rad1 (**B**) or Rad10 (**C**). Yeast strains carrying N-terminal HA-tagged versions of Rad26 (**A**), Rad1 (**B**, right panel) or Rad10 (**C**, right panel), or carrying C-terminal HA-tagged versions of Rad1 (**B**, left panel) or Rad10 (**C**, left panel) were grown in YPD medium at 30°C. Non-tagged (NT) strain was also analyzed (**A-C**). Immunoprecipitated fragments from ChIP experiments were amplified with primers corresponding to selected class II gene promoters (P), UAS (U) or ORFs (O), or class III *RPR1* gene or telomere *TEL1R*. A *GAL1* ORF and a non-transcribed region on chromosome V (IGV) were used as negative controls. Mean values and standard deviation (indicated by error bars) of three independent experiments are shown.

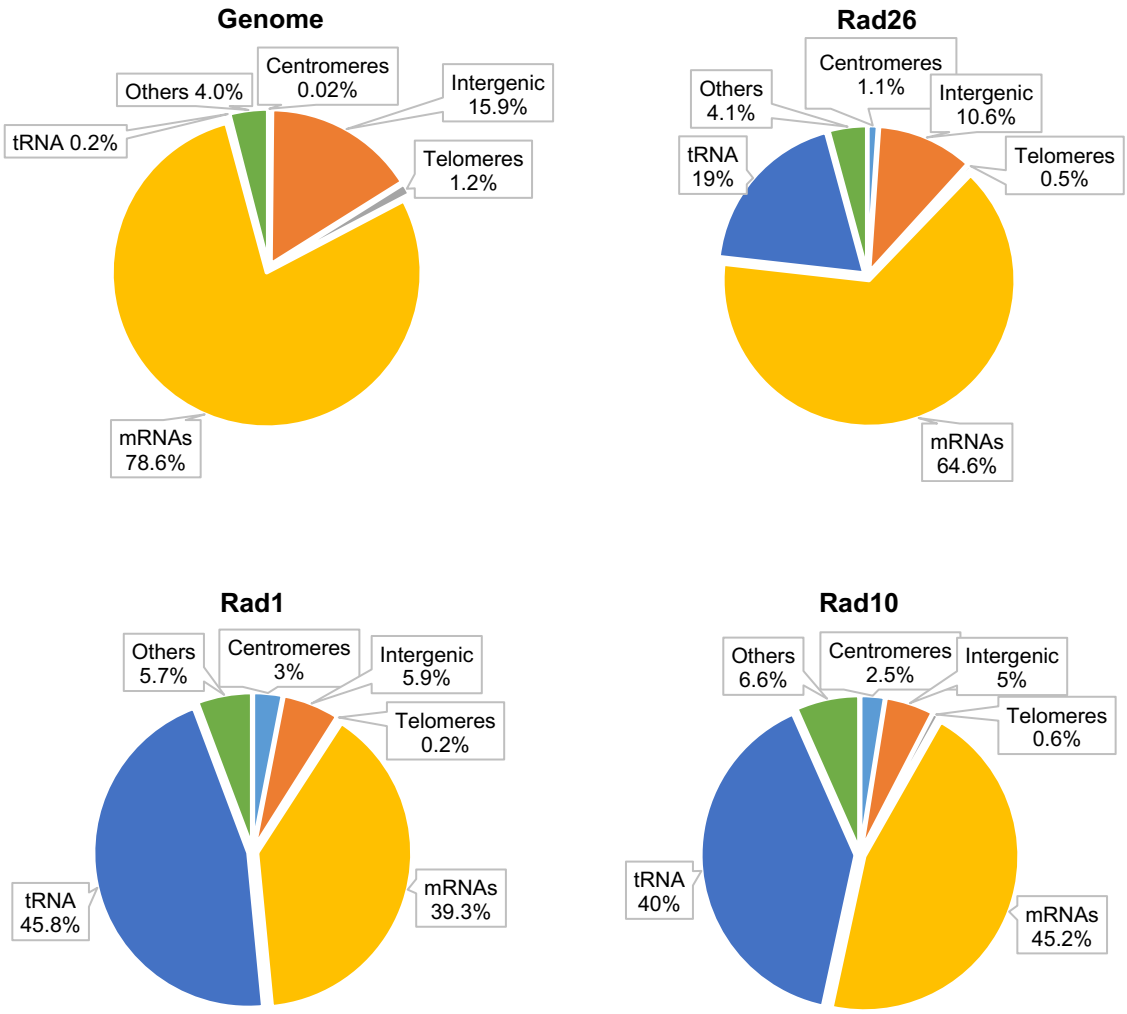

Supplemental Figure S3. Genome-wide analysis of Rad26, Rad1 and Rad10 enrichment peaks.
Pie charts showing the distribution of Rad26, Rad1 and Rad10 enrichment peaks within annotated genomic features including Pol II transcribed regions of protein-coding genes (mRNAs), intergenic regions, telomeres, centromeres, Pol III-transcribed tRNA genes. Proportion of these regions within the yeast genome is also shown.

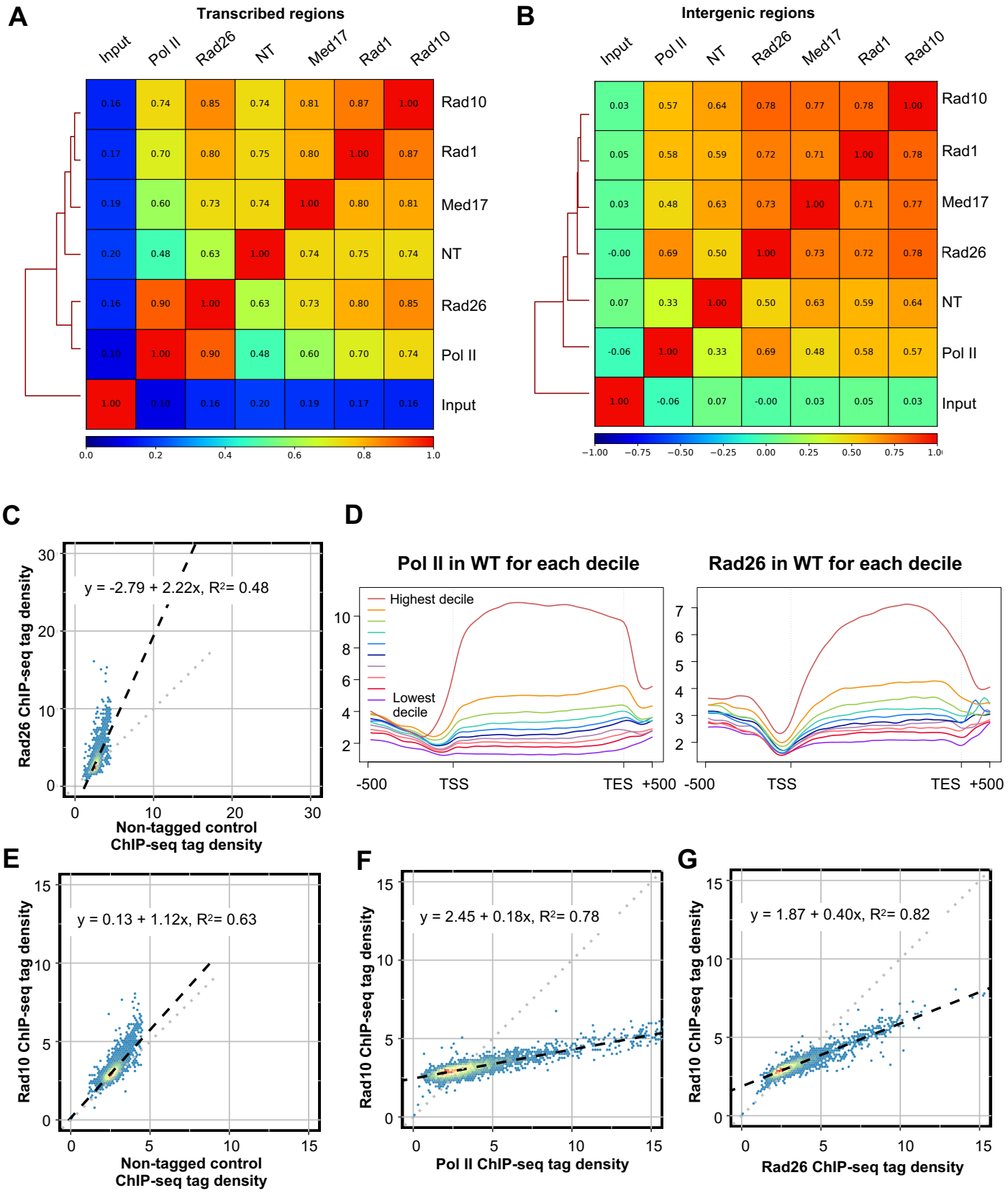

Supplemental Figure S4. Correlation analysis of genome-wide Rad26, Rad1 and Rad10 occupancy.

(**A, B**) Pair-wise Spearman correlation coefficients (SCC) of ChIP-seq data were calculated for Rad1, Rad10, Rad26, Mediator and Pol II in comparison with input and non-tagged controls on Pol II-transcribed regions (**A**) or intergenic regions (**B**). The colors correspond to the scale for SCC indicated on the bottom. (**C-G**) Rad26 ChIP-seq density versus non-tagged control ChIP-seq density (**C**) and Rad10 ChIP-seq density versus non-tagged control ChIP-seq density (**E**) or Pol II ChIP-seq density (**F**) or Rad26 ChIP-seq density (**G**) on Pol II-transcribed genes. Each point on the plot corresponds to one transcribed region. A linear regression (dotted line) and an R^2 linear regression coefficient are indicated. The dashed line corresponds to y = x. (**D**) Average tag density in Rpb1 Pol II ChIP (left panel) and Rad26 ChIP (right panel) in wild type strain on transcribed regions (scaled windows for 500bp before TSS, between TSS and TES, and 500 bp after TES) was calculated for deciles of genes defined according to the Pol II enrichment (from the lowest decile group with lowest enrichment in violet corresponding to 10% lowest Pol II enrichment to a 10th decile group with highest enrichment in red corresponding to 10% highest Pol II enrichment).

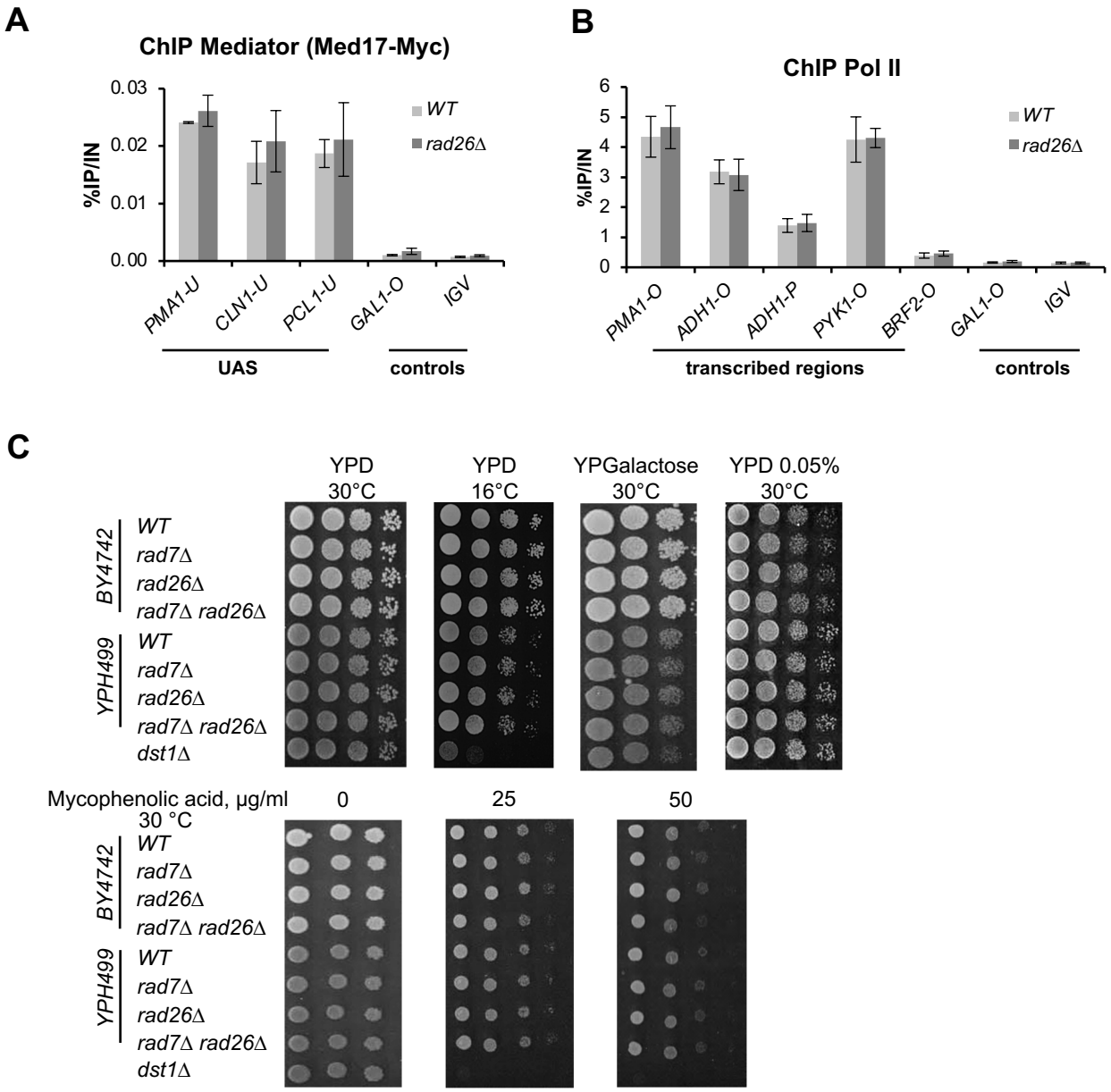

Supplemental Figure S5. Mediator and Pol II occupancy in *rad26*Δ strain and growth phenotypes of *rad26*Δ in GGR-proficient and deficient (*rad7*Δ) context.

(**A, B**) Quantitative ChIP analysis of Mediator (Med17-Myc) and Pol II occupancy was performed with α-Myc antibody against Med17-Myc (**A**) or α-Rpb1 Pol II antibody (**B**) in wild type and *rad26* deletion strains. Immunoprecipitated fragments from ChIP experiments were amplified with primers corresponding to selected class II gene UAS (U) or ORFs (O). A *GAL1* ORF and a non-transcribed region on chromosome V (IGV) were used as negative controls. Mean values and standard deviation (indicated by error bars) of three independent experiments are shown.

(**C**) Growth phenotypes of *rad26*Δ in GGR-proficient and deficient context.

Wild type and isogenic *rad26* deletion strains in GGR-proficient or *rad7* (GGR-deficient) BY4741 and YPH499 contexts were serially diluted, spotted on indicated agar plates, and incubated for 3 days at 30°C. UV-sensitivity assays are shown in **Supplemental Figure S1**. Rich media supplemented with 2 or 0.05% glucose (YPD and YPD 0.05%, respectively), 2% galactose (YPGalactose), minimal SC medium containing indicated concentrations of mycophenolic acid (MPA), were used. *dst1* (TFIIS gene) deletion strain was added for MPA-sensitivity control.

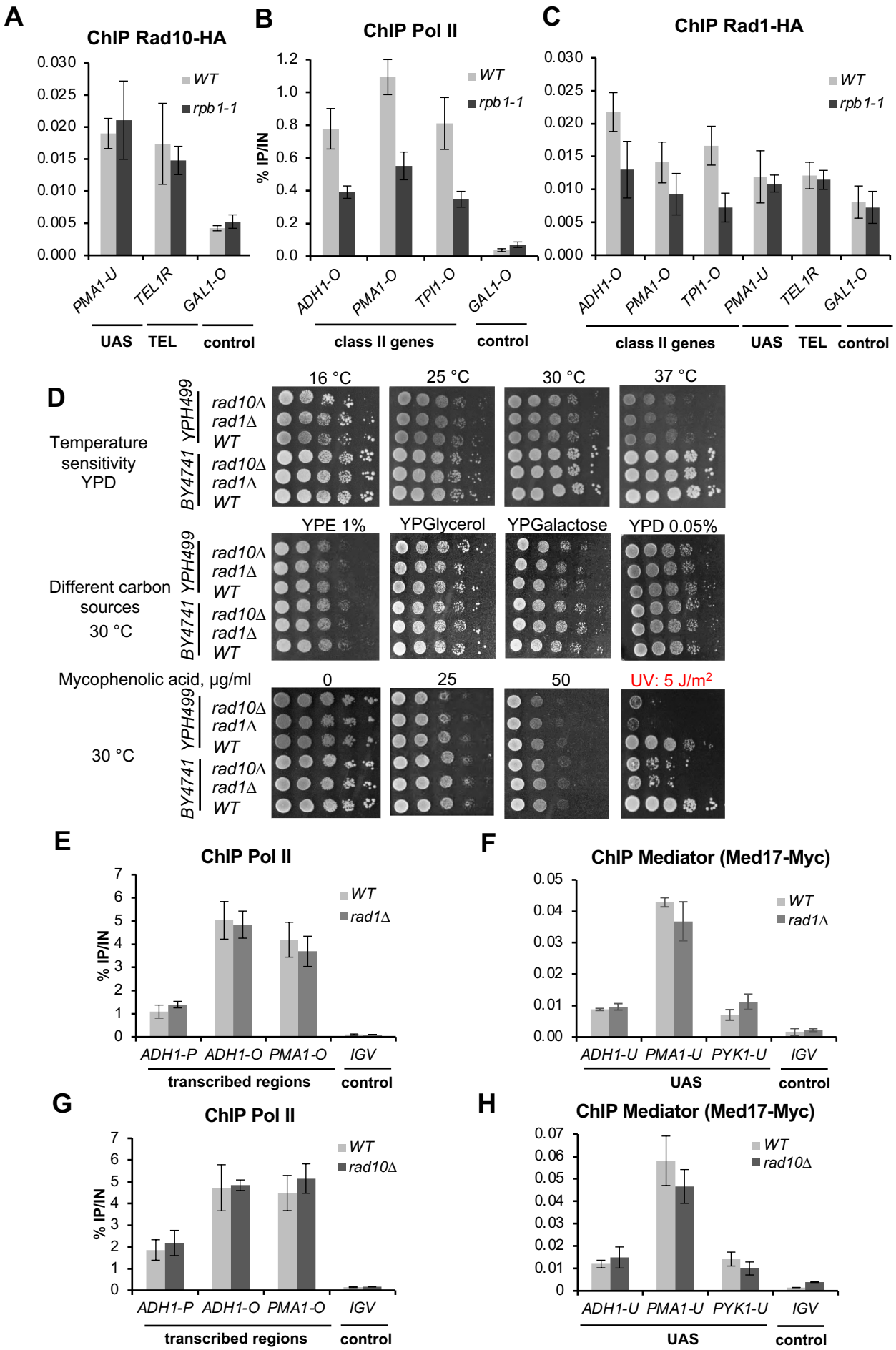

Supplemental Figure S6. Effect of *rpb1-1* mutation on Rad10 occupancy, growth phenotypes of *rad1* and *rad10* deletion strains and ChIP analysis of Pol II and Mediator in these deletion contexts.

(*Continued on the next page*)

(**A-C**) Effect of *rpb1-1* Pol II mutation on Rad10, Rad1 and Pol II occupancies on selected regions. Quantitative ChIP assays were performed using α-Rpb1 antibody (Pol II) (**B**), and α-HA antibody against Rad10-HA or Rad1-HA (**A**, **C**). Cells were grown in selective SD medium complemented with amino acids at 25°C and then shifted for 90 min at 37°C. *GAL1-O* amplicon was used as a negative control. Quantities were normalized to qPCR performed on Input DNA and are expressed as a percentage. The indicated value is the mean of three biological replicates, and error bars represent the standard deviation.

(**D**) Growth phenotypes of *rad1*Δ and *rad10*Δ strains.

Wild-type and isogenic *rad1* and *rad10* deletion strains in BY4741 and YPH499 contexts were serially diluted, spotted on indicated agar plates, and incubated for 3 days at 30°C. For UV-sensitivity assays, cells were treated or not with 5J/m² of UV (UV Stratalinker 1800). Rich media supplemented with 2 or 0.05% glucose (YPD and YPD 0.05%, respectively), 2% galactose (YPGal), 1% ethanol (YPE 1%), 2% galactose (YPGalactose) or 2% glycerol (YPGlycerol), minimal SC medium containing indicated concentrations of mycophenolic acid (MPA), were used. The only observed phenotype of *rad1* and *rad10* deletion strains (UV sensitivity) is highlighted in red.

(**E-H**) Mediator and Pol II ChIP analysis in *rad1* and *rad10* deletion strains at selected regions.

Quantitative ChIP assays were performed using α-Rpb1 antibody (Pol II) (**E, G**), and α-Myc antibody against Med17-Myc (**F, H**). Wild-type and *rad1* (**E, F**) or *rad10* (**G, H**) deletion strains were grown in rich YPD medium at 30°C. A non-transcribed region on chromosome V (IGV) amplicon was used as a negative control. Quantities were normalized to qPCR performed on Input DNA and are expressed as a percentage. The indicated value is the mean of three biological replicates, and error bars represent the standard deviation.

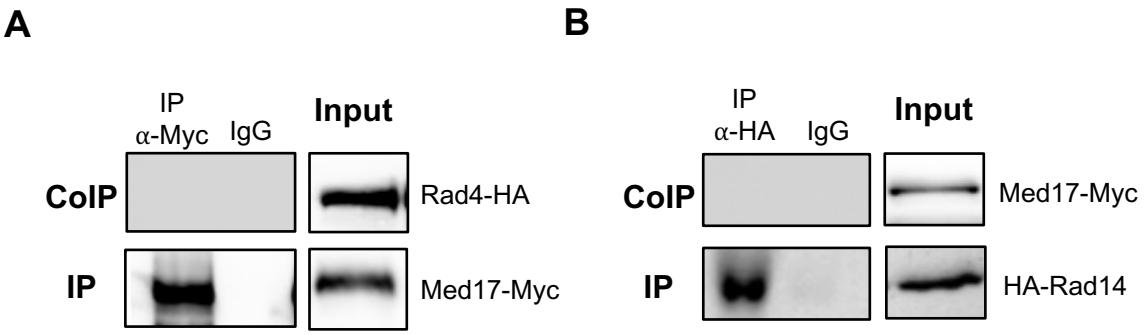

Supplemental Figure S7. No coimmunoprecipitation between Mediator and Rad4 or Rad14.

(**A**) Mediator was immunoprecipitated from crude yeast extracts via Med17-Myc subunit with α-Myc antibody (IP) and Western blotting with α-HA antibody detected Rad4-HA (CoIP).

(**B**) HA-Rad14 was immunoprecipitated with α-HA antibody from crude yeast extracts and analyzed by Western blotting with α-Myc antibody against Med17-Myc Mediator subunit. No coimmunoprecipitation with Med17 Mediator subunit was detected (CoIP) (left panels). IgG indicates a control immunoprecipitation with IgG magnetic beads only. Inputs are shown on right panels.

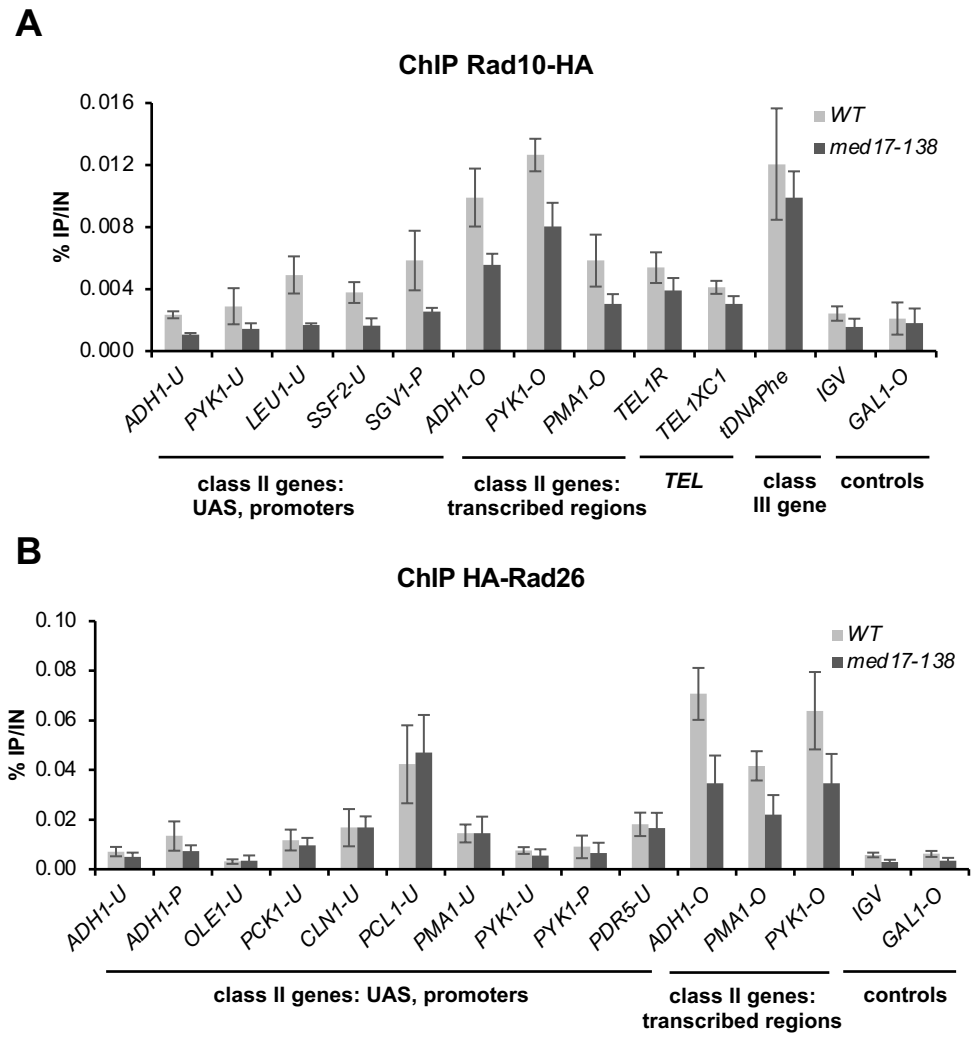

Supplemental Figure S8. Effect of the *med17-138* mutation on Rad10 and Rad26 occupancies at selected regions.

Quantitative ChIP assays were performed using α-HA antibody against Rad10-HA (**A**) or HA-Rad26 (**B**). Cells were grown in selective SD medium complemented with amino acids at 25°C and then shifted for 45 min at 37°C. *GAL1-O* and *IGV* (non-transcribed region on chromosome V) amplicons were used as negative controls. Quantities were normalized to qPCR performed on Input DNA and are expressed as a percentage. The indicated value is the mean of three biological replicates, and error bars represent the standard deviation.

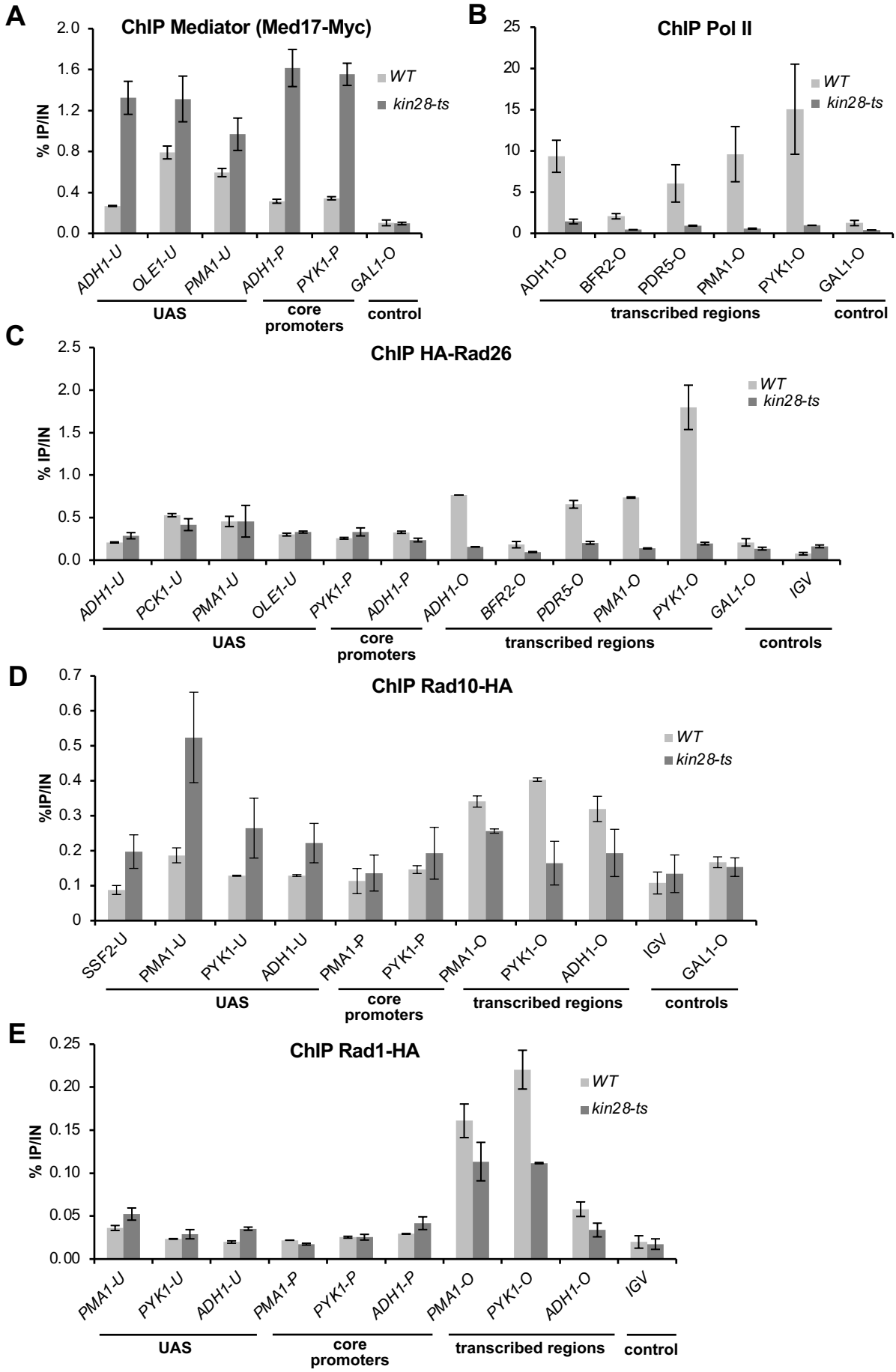

Supplemental Figure S9. Rad26, Rad1, Rad10 ChIP analysis in comparison with Pol II and Mediator (Med17-Myc) in the *kin28* mutant. Quantitative ChIP analysis of Mediator (Med17-Myc), Pol II, HA-Rad26, Rad10-HA and Rad1-HA occupancy was performed with α-Myc antibody against Med17-Myc (**A**), α-Rpb1 Pol II antibody (**B**) or α-HA antibody against HA-Rad26 (**C**), Rad10-HA (**D**) and Rad1-HA (**E**) in wild type and *kin28-ts* strains. Cells were grown in selective SD medium complemented with amino acids at 25°C and then shifted for 75 min at 37°C. Immunoprecipitated fragments from ChIP experiments were amplified with primers corresponding to selected class II gene UAS (U), promoters (P) or ORFs (O). A *GAL1* ORF and a non-transcribed region on chromosome V (IGV) were used as negative controls. Mean values and standard deviation (indicated by error bars) of three independent experiments are shown.

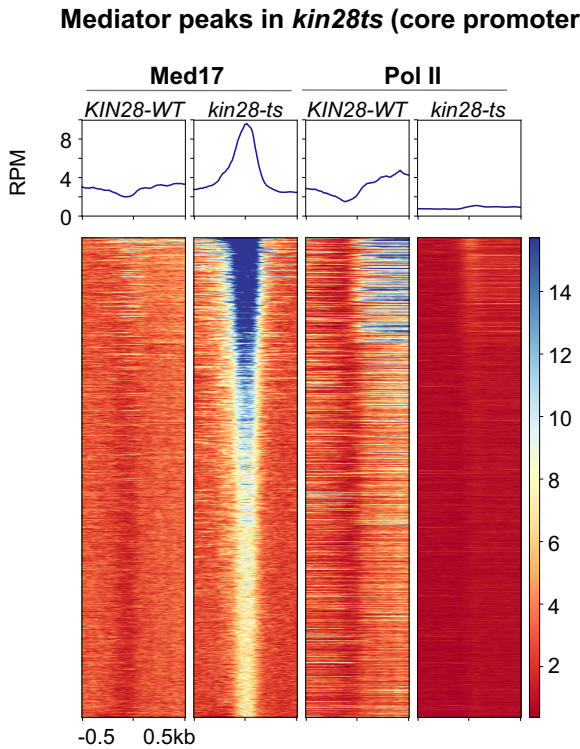

Supplemental Figure S10. Effect of the *kin28-ts* mutation on genome-wide Mediator and Pol II occupancy.

Heat maps of Mediator (Med17) and Pol II ChIP-seq profiles centered on Mediator (Med17) enrichment peaks determined in the *kin28-ts* mutant (core promoters, -500 bp to +500 bp), sorted by decreasing Mediator occupancy. Wild type and *kin28-ts* strains were compared. Median tag density profiles in RPM (reads per million) are shown in upper panels.

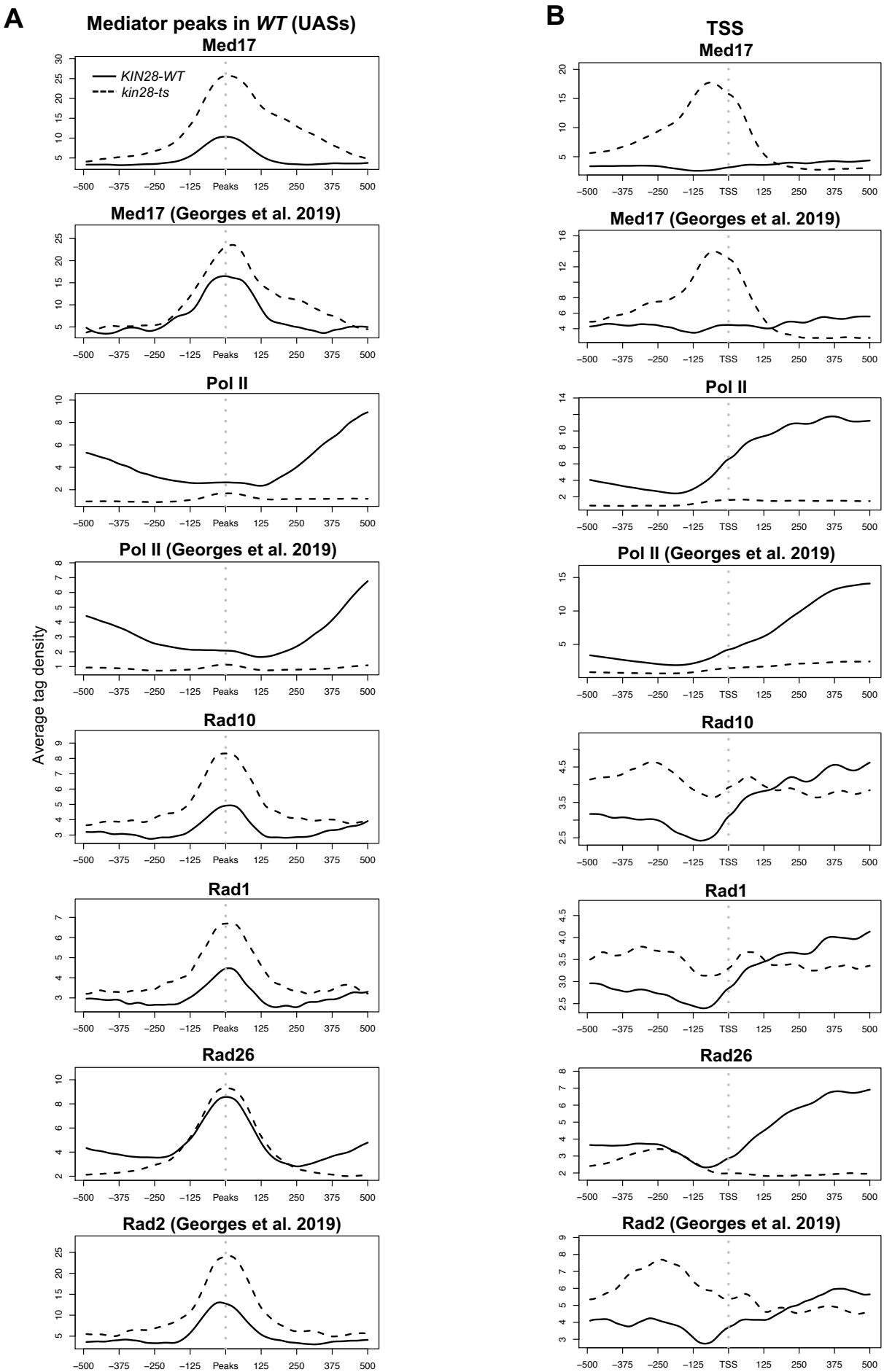

Supplemental Figure S11. Metagene analysis of genome-wide Mediator, Pol II, Rad26, Rad1, Rad10 and Rad2 occupancy on Mediator enrichment peaks in the wild type strain (UASs) and around TSS.

Average tag density in wild type (WT) strains is indicated as a full line, whereas average tag density in *kin28-ts* strains is indicated as a dashed line. Average tag density in Med17 Mediator, Pol II, Rad26, Rad1 and Rad10 ChIP around Med17 Mediator enrichment peaks (-500 bp to +500 bp) determined in the wild type (WT) strain corresponding to UASs (**A**) or centered on TSS (-500 bp to +500 bp) (**B**). For comparison, ChIP-seq data for Med17 Mediator, Pol II and Rad2 from our previous work were also included (Georges et al. 2019).

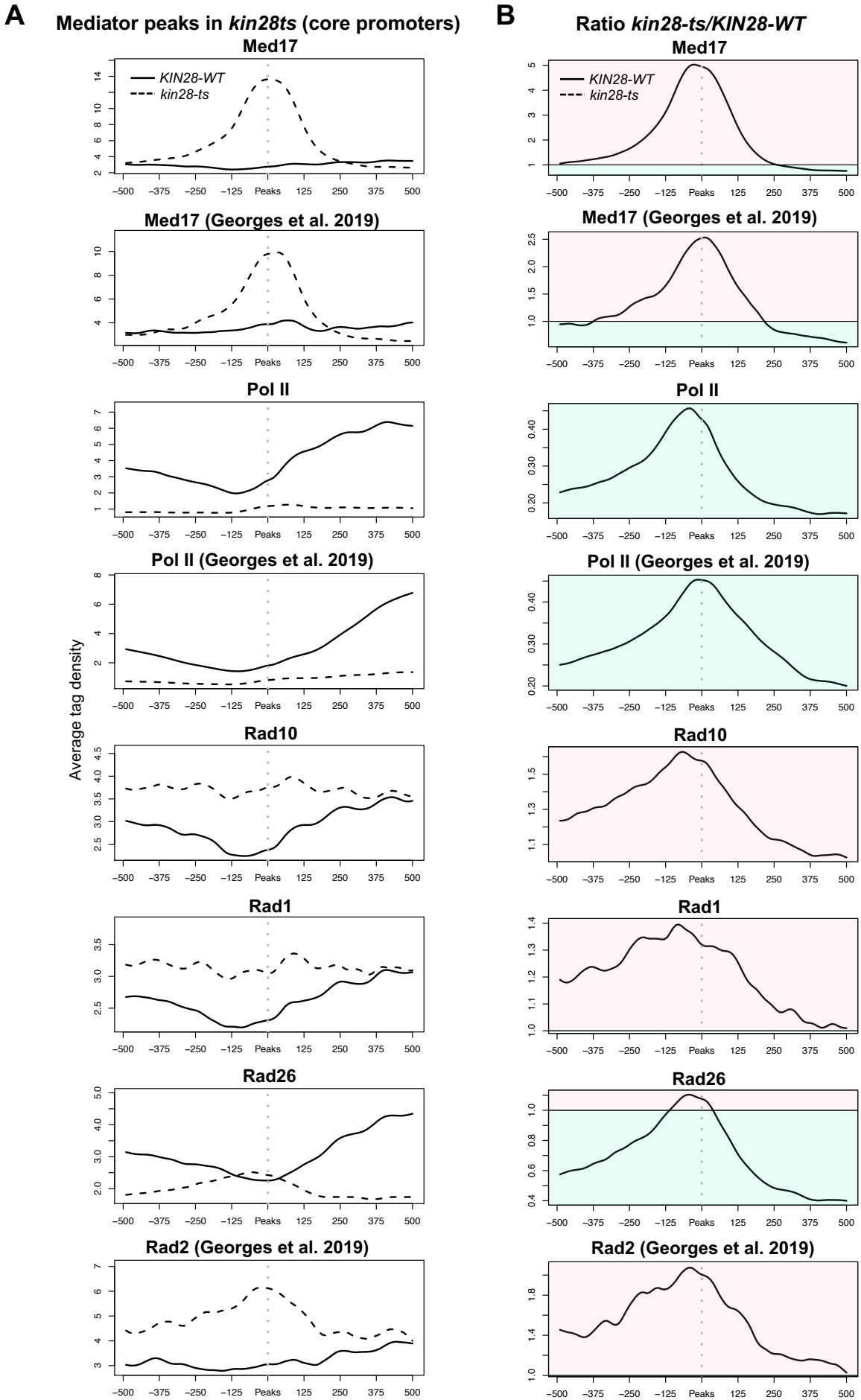

Supplemental Figure S12. Metagene analysis of genome-wide Mediator, Pol II, Rad26, Rad1, Rad10 and Rad2 occupancy on Mediator enrichment peaks in *kin28-ts* strains (core promoters).

Average tag density in wild type (WT) strains is indicated as a full line, whereas average tag density in *kin28-ts* strains is indicated as a dashed line. Average tag density (**A**) or ratio between the *kin28-ts* mutant and the wild type (**B**) for Med17 Mediator, Pol II, Rad26, Rad1 and Rad10 ChIP around Med17 Mediator enrichment peaks (-500 bp to +500 bp) determined in *kin28-ts* strain corresponding to core promoters. For comparison, ChIP-seq data for Med17 Mediator, Pol II and Rad2 from our previous work were also included (Georges et al. 2019).

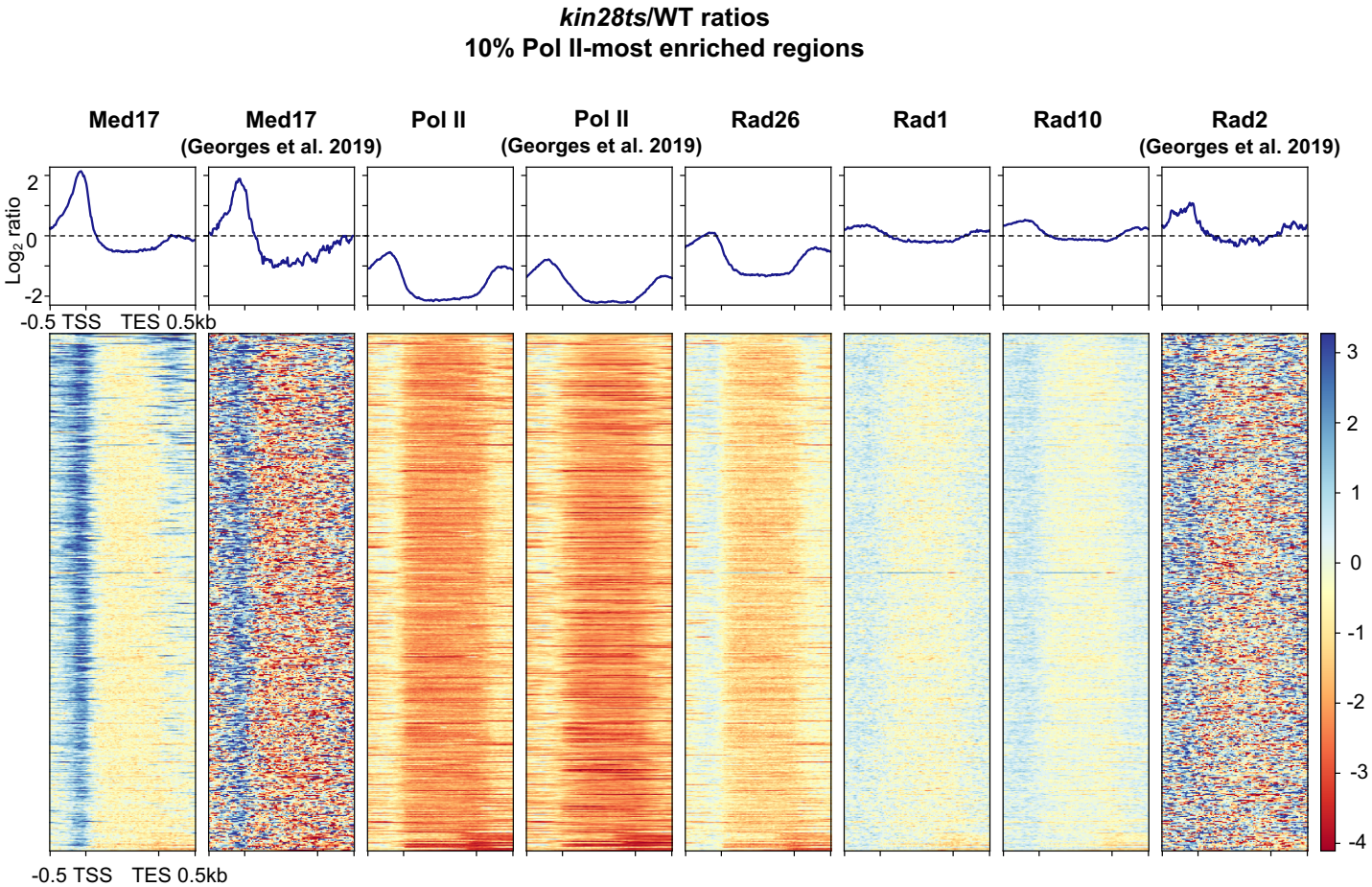

Supplemental Figure S13. Metagene analysis of genome-wide Mediator, Pol II, Rad26, Rad1, Rad10 and Rad2 occupancy on transcribed regions in wild type and *kin28-ts* strains.

Med17 Mediator, Pol II, Rad26, Rad1 and Rad10 ChIP occupancy ratios between the *kin28-ts* mutant and the wild type on 10% Pol II-most enriched regions (scaled windows for 500 bp before TSS, between TSS and TES, and 500 bp after TES). For comparison, ChIP-seq data for Med17 Mediator, Pol II and Rad2 from our previous work were also included (Georges et al. 2019).

A

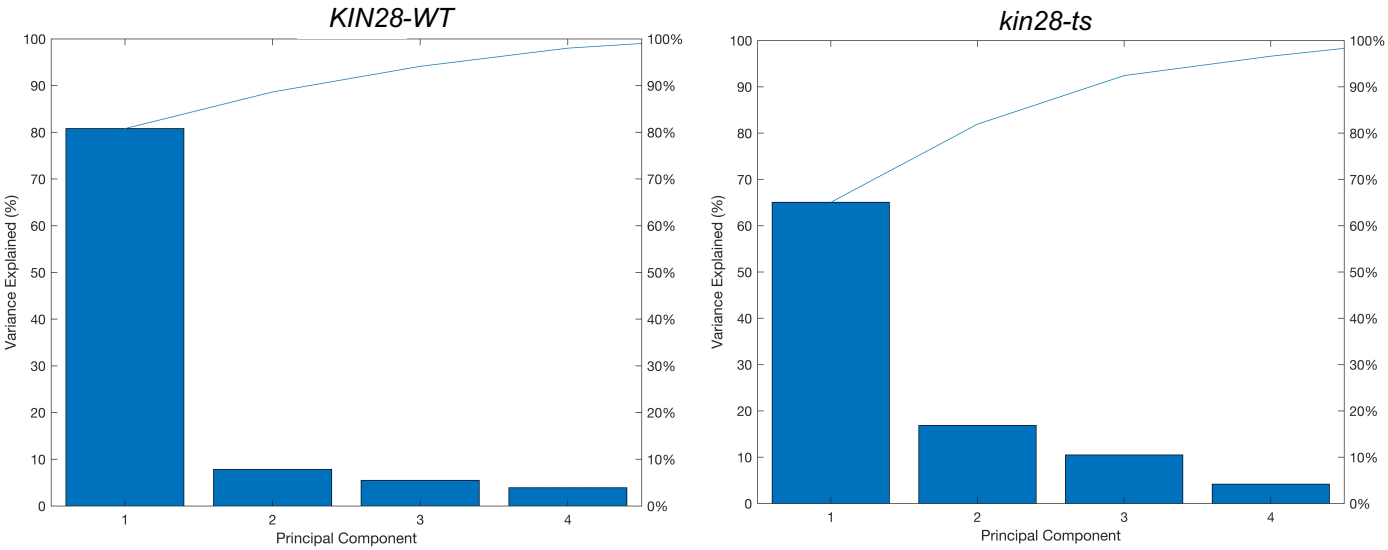

B

	Norms *KIN28-WT*	Norms *kin28-ts*
Med17	0.905	0.827
Pol II	0.738	0.924
Rad10	0.566	0.612
Rad1	0.723	0.745
Rad26	0.890	0.729

C

	PC1 *KIN28-WT*	PC1 *kin28-ts*	PC2 *KIN28-WT*	PC2 *kin28-ts*	PC3 *KIN28-WT*	PC3 *kin28-ts*
Med17	0.465	0.493	**-0.880**	**0.749**	-0.098	0.442
Pol II	0.595	0.439	**0.764**	0.519	0.251	**-0.733**
Rad10	**0.834**	**0.798**	0.105	-0.599	**-0.5421**	0.062
Rad1	**0.634**	0.598	0.273	**-0.658**	**-0.723**	-0.457
Rad26	0.499	**0.660**	-0.078	-0.141	**0.863**	**0.738**

Supplemental Figure S14. PCA of Mediator, Rad1, Rad10, Rad26 and Pol II ChIP-seq data on intergenic regions.

(**A**) Pareto chart of the distribution of sample variance as a function of number of principle components (PCs) in wild type (left panel) or *kin28-ts* (right panel) contexts. The histogram represents the explained variance in percentage (y-axis) for each PC (x-axis) and the line corresponds to the total variance explained by 1 to 4 PCs.

(**B**) Norms of each variable Med17 (Mediator), Pol II, Rad1, Rad10 and Rad26 in the orthonormal referential of 3PCs for wild type and *kin28-ts* strains.

(**C**) Contribution of each variable to each PC (PC1, 2 and 3) in wild type and *kin28-ts* strains. The values for main contributors are indicated in bold.

A ***KIN28-WT, intergenic regions***

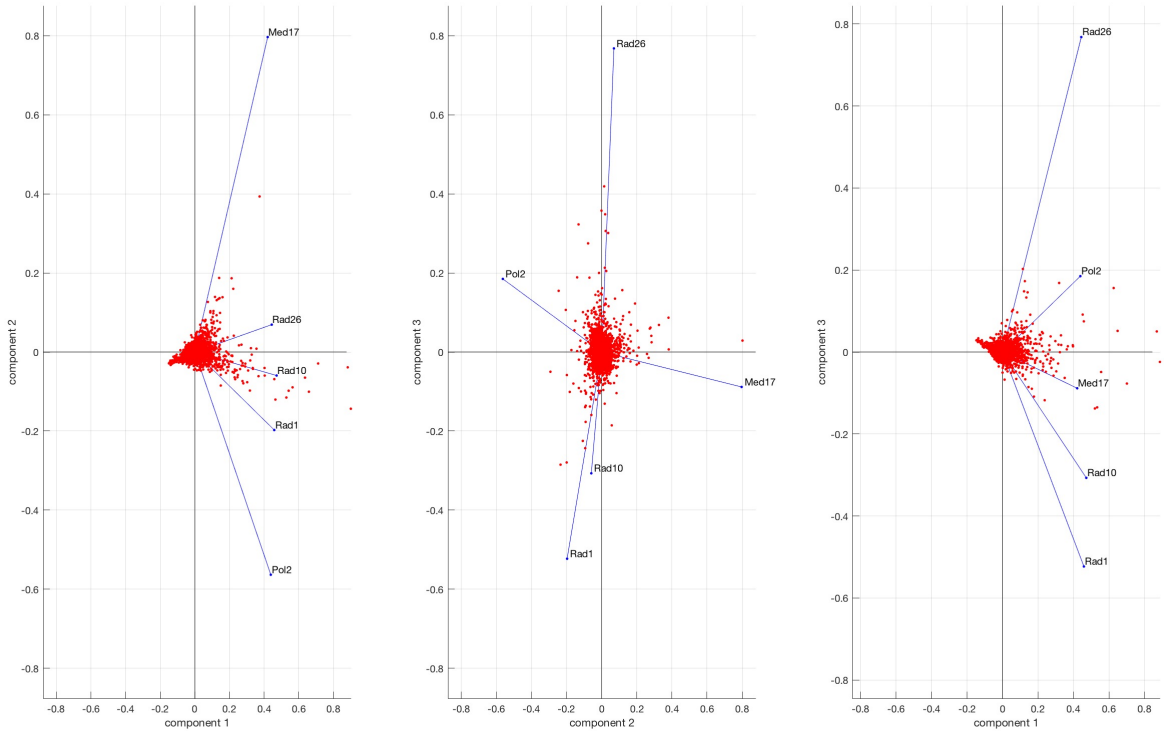

B ***kin28-ts, intergenic regions***

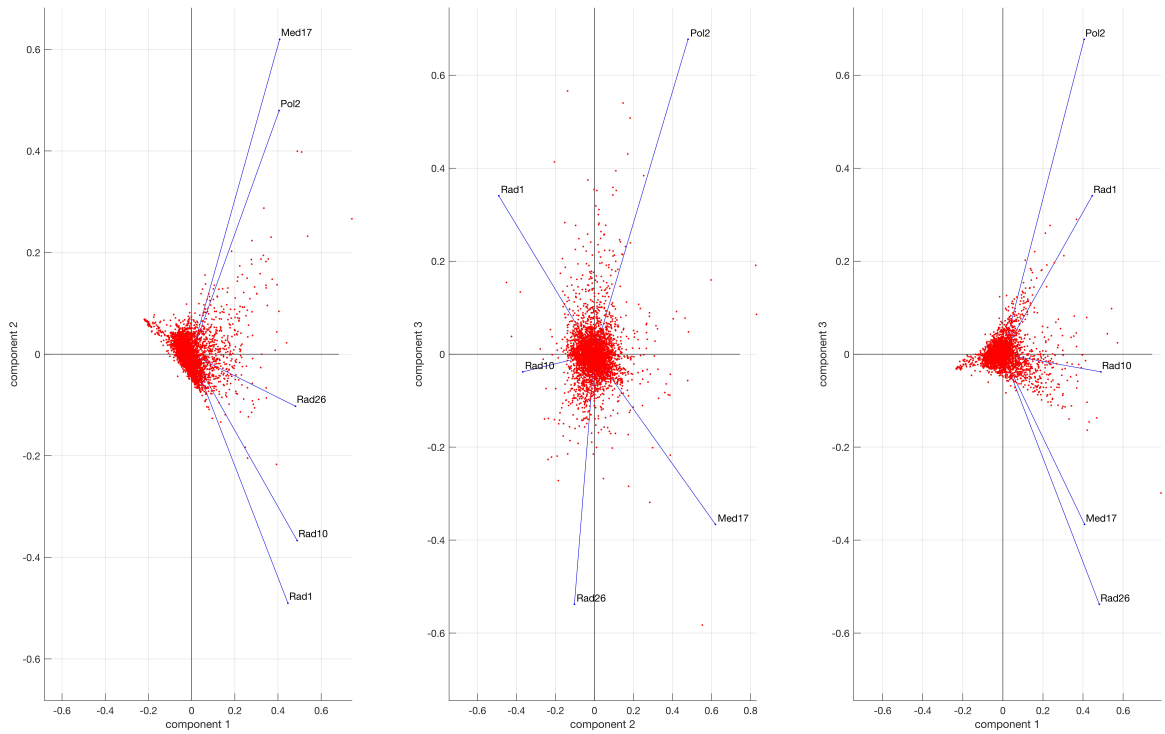

Supplemental Figure S15. Projections of Mediator, Rad1, Rad10, Rad26 and Pol II ChIP-seq data on 2 PCA plane.

Covariance of the variables Mediator (Med17), Pol II, Rad1, Rad10 and Rad26 for ChIP-seq data in intergenic regions were projected on 2 PCA axes (PC1 versus 2, PC2 versus 3, PC1 versus 3) in wild type (**A**) or *kin28-ts* (**B**).

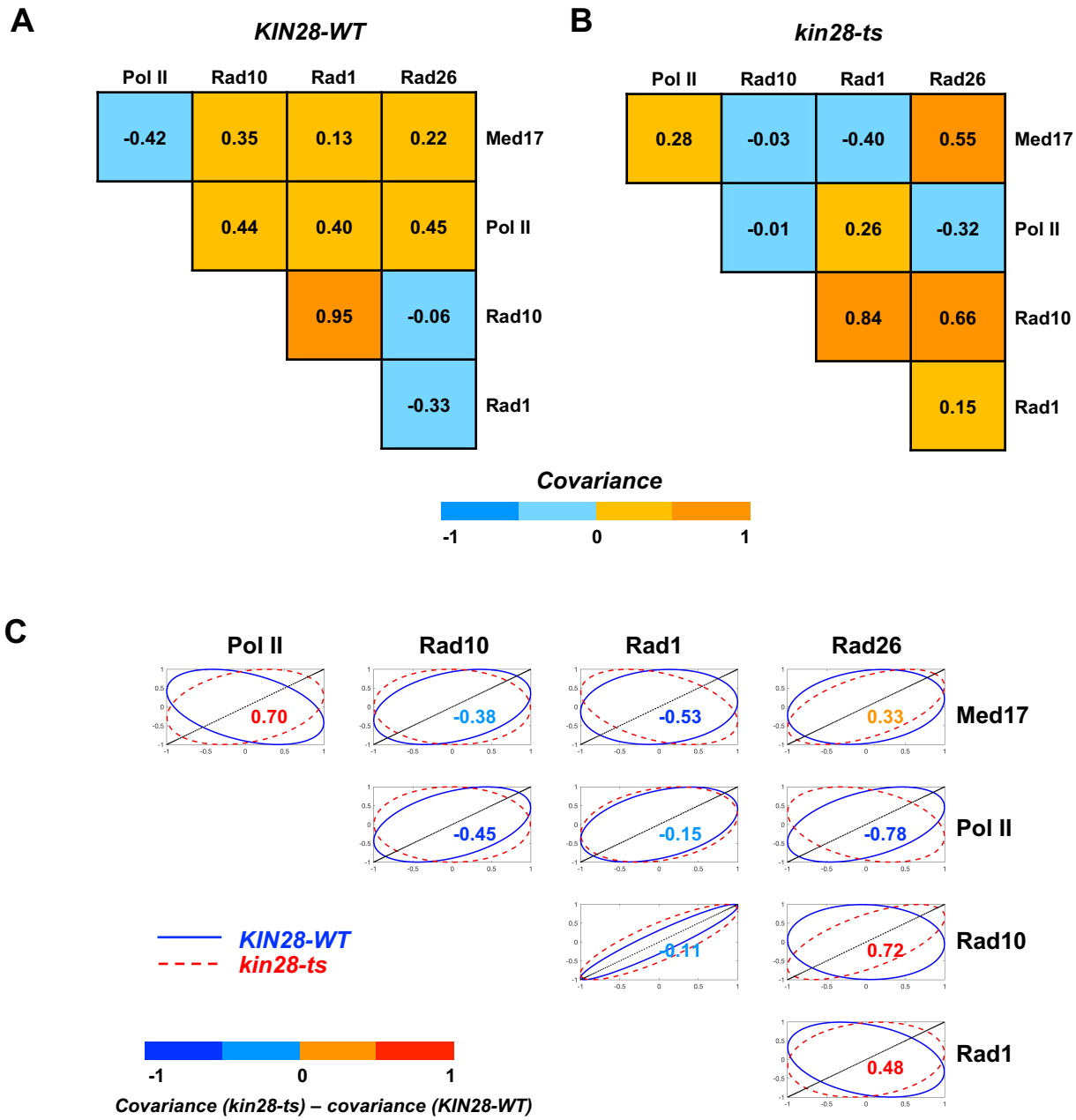

Supplemental Figure S16. Multivariate analysis of the relationship between Mediator, Rad1, Rad10, Rad26 and Pol II.

Covariance of the variables Mediator (Med17), Pol II, Rad1, Rad10 and Rad26 for ChIP-seq data on intergenic regions in wild type (*KIN28-WT*) (**A**) or *kin28-ts* (**B**) calculated as described in M&M. Covariance in the wild type and the mutant are indicated according to the 4-color code (from light blue (-1) to orange (1)).

(**C**) Comparison of the covariance distribution of the variables Mediator (Med17), Pol II, Rad1, Rad10 and Rad26 for ChIP-seq data on intergenic regions in wild type (*KIN28-WT,* blue contour) or *kin28-ts* (red contour) calculated as described in M&M. The width of the ellipsoid (small radius) corresponds to the dispersion of the relation between the two variables. The differences of covariance between the wild type and the mutant are indicated within each ellipsoid according to the 4-color code (blue, light blue, orange, red, from -1 to 1).